Wood and Delignified Wood for Shape-Stabilized Phase-Change Materials in Application to Thermal Energy Storage

Wood and Delignified Wood for Shape-Stabilized Phase-Change Materials in Application to Thermal Energy Storage

Amelia Carolina Sparavigna

Department of Applied Science and Technology, Polytechnic University of Turin, Italy

Email: amelia.sparavigna@polito.it

Abstract

Thousands of years have seen the wood used for many fundamental purposes, as a fuel or as a material for building houses or for creating tools and furniture. Today, many researches aim to improve the properties of this traditional material for further innovative applications. Here we will consider the enhancement of the wood thermal features by means of its impregnation with phase-change materials (PCMs). A PCM is a substance absorbing and releasing thermal energy at a phase transition. Therefore, wood and PCMs can be composed to be useful for the thermal energy storage, that is for heating and cooling applications. Here we propose a discussion of recent literature about development and application of wood-based composite PCMs. In particular, we will consider the delignified wood. With delignification, the density and chemistry of wood can be altered, obtaining a scaffold possessing an enhanced porosity suitable for an improved impregnation with PCMs. Regarding the effect of the size of pores in wood, a discussion about the depression of the melting temperatures in composite PCMs is also provided.

Keywords: Phase Chance Materials, Shape Stabilized Phase Change Materials, Wood, Delignified Wood, Transparent Wood, Biochar, Composite Materials, Biomass Based Porous Carbon, Phase Change Composites, Thermal Management, Thermal Conductivity, Latent Heat Storage Biocomposites, Gibbs Thomson Equation, Gibbs composite-system thermodynamics, Melting and freezing temperature depression.

Subject Areas: Materials Science.

Submitted SSRN - January 4, 2023

Introduction

Wood has been used for thousands of years as a fuel or as a material for building houses or creating tools and furniture. Today research aims to improve properties of wood for traditional uses, its stability when wood is subjected to fluctuations of moisture content or its resistance to the biodegradation provoked by microorganisms, besides finding new applications for such a fundamental material (Spear et al., 2021, Blanchet & Pepin, 2021). Nanotecnologies are required by this research too, because they can offer methods to improve the wood characteristics. In fact, the intrinsic porosity of wood reaches the nanometric scale, that is the scale of the small-sized particles used in nanotechnologies (Papadopoulos et al., 2019). Porosity is also fundamental for the enhancement of wood thermal properties by means of its impregnation with phase-change materials (PCMs), and this is the subject of the present discussion.

A phase-change material, PCM, is a substance which is able of absorbing and releasing energy at phase transitions, finding its natural use in heating and cooling applications (Du et al., 2018). By melting and solidifying at a given temperature, a phase-change material is able to store or release energy. Being the transition of the first order (Binder, 1987), the PCM is also considered as a "latent heat storage" (LHS) material. An example of LHS material is the ice (specific heat of fusion, 333.55 J/g). Water/ice is therefore a PCM, which can be used to store winter cold to cool buildings in summer (Sparavigna et al., 2011).

In the last few decades, several substances such as hydrocarbons (Daniarta et al., 2022) and paraffins (Akgün et al., 2007) have been adapted to produce PCMs suitable to have several different phase transition temperatures. This research approach produced a consequently expanded temperature range of PCMs which can be relevant for applications in the huge potential market of heating and cooling buildings (Zhang et al., 2006, Sivanathan et al., 2020). In this framework, besides the wood for the wood-based composite PCMs, other materials are under investigation such as biochar (Zhang et al., 2022a). Biochar is the fine-grained residue of the pyrolysis of biomass. It is the product of the thermochemical decomposition at moderate temperatures (350-700°C) under oxygen-limiting conditions (Brassard et al., 2019). The principal use of biochar is as amendment in agricultural soils, because of its high carbon content, stability, porosity and surface area (Singh et al., 2010, Brassard et al., 2019, Ok et al., 2015, 2018, Bates & Draper, 2019). However, due to its functional surface, biochar is exhibiting high compatibility with cement, asphalt and polymer (Bartoli et al., 2019, 2020, 2022, Panahi et al., 2020, Rosso et al., 2020, Danish et al., 2021, Das et al., 2021, Maljaee et al., 2021, Tan et al., 2021, Lepak-Kuc et al., 2021, Minugu et al., 2021, Sirico et al., 2021, Hernandez-Charpak et al., 2022, Kane, 2022, Jiang et al., 2022, Suarez-Riera et al., 2022).

In a recent discussion (Sparavigna, 2022), we have considered the use of biochar in shape-stabilized PCMs (SSPCMs), in particular for organic PCMs. These PCMs are widely used because of their properties: a proper transition temperature, a high latent heat and thermal and chemical stability (Rathod & Banerjee, 2013, Jebasingh & Arasu, 2020). The shape stabilization is solving the main disadvantage of these materials, which is their liquid flow and consequent leakage in the phase-change temperature range. To avoid the leakage problem, some solutions have been proposed. The solutions can be subdivided in encapsulation and shape-stabilization (Khadiran, et al., 2015, Abdeali et al., 2020). The encapsulation - let's say, the "true" encapsulation - is based on the specific creation of a capsule shell for the PCM. The shape-stabilization is based on the use of a porous material (such as biochar for instance), which is infiltrated by the fluid. Sometimes, the shape-stabilization is also simply defined as an "encapsulation".

In the review by Trisnadewi and Putra, 2020, SSPCMs for thermal energy storage are considered in general. The thermal energy storage (TES) can mitigate the increasing energy consumption, but TES requires improved composites, able to store *large* amounts of thermal energy in *small* volumes. SSPCM can be obtained by vacuum impregnation, a method which is also removing gas and moisture from the pores of the supporting material. In the article by Zhang et al., 2006, the preparation and thermal performance of SSPCMs have been considered. At the time, 2006, the authors told that SSPCM was "a kind of *novel* PCM". The salient feature is: "keeping shape stabilized in the phase change process and *no need* for containers" (Zhang et al., 2006). As told by Zhang and coworkers, polymeric matrices have been generally used to shape stabilize the paraffin. Today, biochar is also considered for the same purpose. Here, we are interested to the use of wood-based composites in order to shape-stabilize PCMs in the porous structure of the wood.

Hard and soft

When observed by means of a microscope, wood reveals itself as composed of cells. The basic cell types are: tracheids, vessel members, fibres and parenchyma (Tsoumis, 1991). Wood is distinguished in softwood, where cells are tracheids and parenchyma, and in hardwood, where there are vessel members, fibres and parenchyma. A few hardwood species contain tracheids too. The tracheids are the type of the cells that, after evolution, produced vessel members and fibres. The softwood is mainly composed by tracheids, primarily arranged in axial mode; hardwood has vessel members and fibres axially oriented (Tsoumis, 1991). The wood cells are tubelike, but tracheids and fibres have their ends which are closed, whereas the vessel members have ends which are wholly or partly open. The vessel members are connected to form axial pipelines, the vessels, of indeterminate length. The "pores" that we can see in the section of hardwood are the vessel members. Axial tracheids and vessel members are the principal cells for water conduction. The main function of fibres is that of providing mechanical support. Parenchyma cells are concerned with storage and transport of food (Tsoumis, 1991).

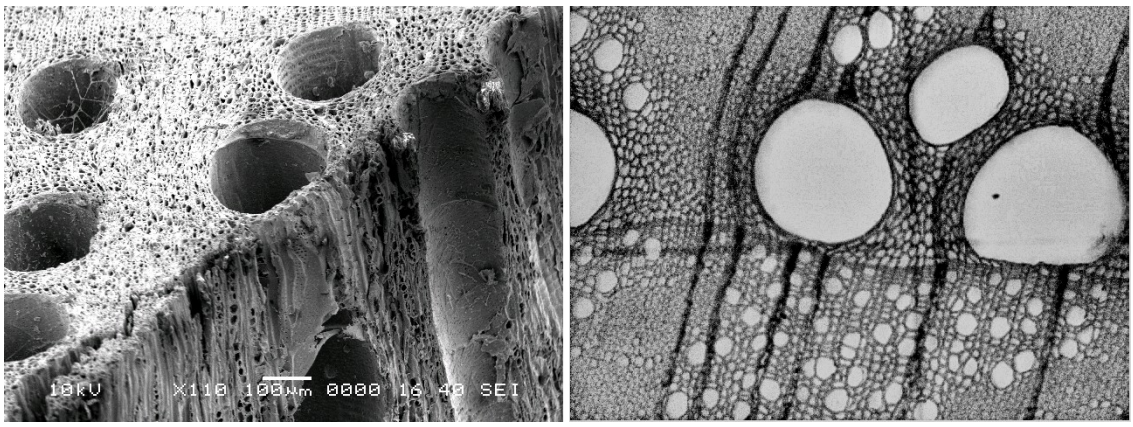

Figure 1 - Scanning electron microscope image (left) and transmission light microscope image (right) of vessel elements in oak. Courtesy McKDandy (the author) at English Wikipedia. The file is licensed under the Creative Commons Attribution-Share Alike 3.0 Unported, as declared at https://commons.wikimedia.org/wiki/File:Hardwood_Pores.jpg https://web.archive.org/web/20221229075329/https://commons.wikimedia.org/wiki/File:Hardwood_Pores.jpg

The wood cells are made of cell wall and cell cavity. Dead cells have the cavity which is empty. In the cell walls, we can find gaps of various shapes, defined as "pits". Pits are passages between adjacent cells. Other microscopic features are tyloses, plugs that are obstructing the vessel members of hardwoods. Tyloses are formed when the sapwood is transformed into heartwood.

As told by George Tsoumis in Britannica, the cell walls are composed by three layers. It is also stressed that smallest building units of cell walls, visible by microscopes, are the microfibrils. They appear string-like under electron microscope, with a diameter of 10–30 nanometres, but indeterminate

length. The microfibrils are constituted by the chain-like cellulose molecules and are creating the wood skeleton. Hemicellulose, lignin, and pectic substances are non-cellulose components which are located among the microfibrils. These substances are not forming the microfibrils. The lignin is concentrated in the layer separating adjacent cell walls. The proportion of cellulose and other constituents are: cellulose 40–50%, percentage about the same in soft- and hard-wood, hemicellulose 20% in softwood and 15–35 % in hardwood, lignin 25–35% in softwood and 17–25% in hardwood, and pectic substances in very small percentage.

Tsoumis is also mentioning the physical properties of wood. Let us consider those related to the thermal properties. First, wood can expand and contract due to temperature variation, but the related dimensional changes are small when compared to shrinkage and swelling produced by the variation of the moisture content in the wood. Wood has a low thermal conductivity and therefore is considered a thermal insulating material. The thermal conductivity is anisotropic, and larger in the axial direction. It depends on the density and moisture content of wood. Therefore, dry light-wood is a better thermal insulator.

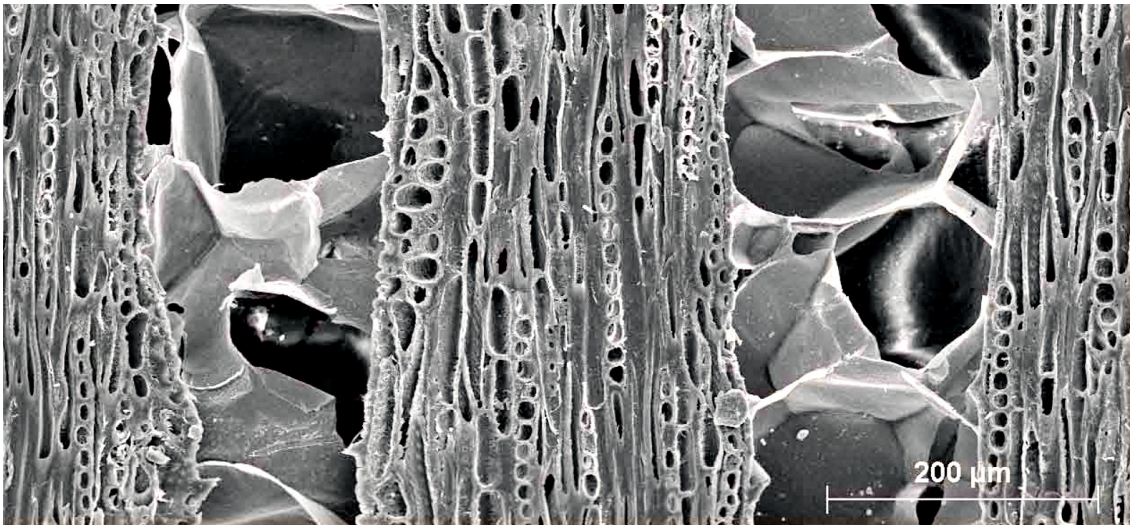

Figure 2 - Vessels of Quercus petraea with tyloses. A detail of an image courtesy of the author Dr. Michael Rosenthal,Technische Universität Dresden (Rosenthal & Bäucker, 2013). The file is licensed under the Creative Commons Attribution-Share Alike 3.0 Unported license, as declared at https://en.wikipedia.org/wiki/File:Verthyllung_Quercus_petraea.jpg https://web.archive.org/web/20221229080024/https://en.wikipedia.org/wiki/File:Verthyllung_Quercus_petraea.jpg

Pores in wood

Before discussing the wood-based composite PCMs, let us talk about the pores in wood, that are present at micro-, meso- and macroscales. A detailed investigation was given by Plötze and Niemz (2011). The researchers measured the porosity of soft- and hardwood with pycnometric methods and mercury intrusion porosimetry (MIP). They observed a great variability in the bulk density, specific

surface area and porosity. Considering the pore size distribution, Plötze and Niemz identified four pore size classes, that they distinguished as micropores (radius 1.8–80 nm), mesopores (radius 80–500 nm) and macropores (radius 0.5–2 μm and 2–58 μm). The micropores are the microvoids or cell wall capillaries. The classification of pores by Plötze and Niemz is different from that given by the International Union of Pure and Applied Chemistry (IUPAC) for porous materials, and based on the pore sizes: microporous, less than 2 nm, mesoporous, from 2 nm to 50 nm, macroporous, greater than 50 nm (Fang et al., 2010). Pore size is generally the distance between two opposite walls of the pore and therefore the diameter in the case of cylindrical pores (Sing, 1991, Salamon, 2014).

Another approach to the wood pore diameters is given by Eric Meier in the Hardwood Anatomy. Meier considers the pores the diameters of which are measured in micrometers. For visual inspection by means of a microscope, it's "more helpful" to "gauge the pore sizes in comparative terms", and then the pores are subdivided in "small" (less than 50 μm)."medium" (in the interval 50-100 μm), "large" (100-200 μm) and "very large" (greater than 200 μm).

Here we will consider the IUPAC classification.

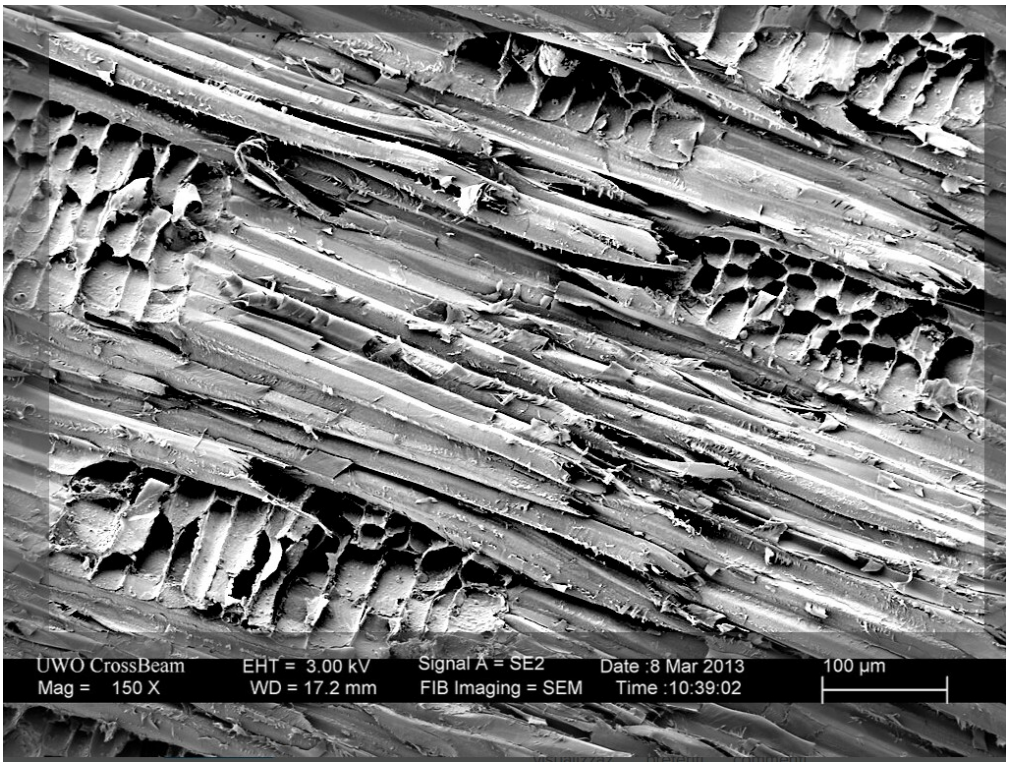

Figure 3 - Wood in a scanning electron microscope image. The wood is Toona Mahogany (Toona Ciliata). The image is a courtesy of the author Todd Simpson, UWO Nanofabrication Facility, license Attribution-NonCommercial-NoDerivs 2.0 Generic (CC BY-NC-ND 2.0) , as declared at https://www.flickr.com/photos/zeissmicro/12695722793, archived at https://web.archive.org/web/20221229080531/https://www.flickr.com/photos/zeissmicro/12695722793

Hierarchy

Let us go "beyond what meets the eye" (Toumpanaki et al., 2021). Toumpanaki and coworkers are talking about the hierarchical structure of wood, structure which is containing "features at all length scales". The hierarchy is going from tracheids or vessel members, through the microfibrils in the cell walls, down to the molecular scale of cellulose, lignin, and hemicellulose. Toumpanaki et al., 2021, are proposing the discussion of the recent results obtained by advanced imaging techniques. Among the mentioned techniques we can find nuclear magnetic resonance spectroscopy, X-ray imaging, Raman and infrared spectroscopy, besides the confocal, electron and atomic force microscopy (AFM).

About the wood components, Toumpanaki and coworkers tell that the cellulose is aggregated into microfibrils (3–5 nm), which are interacting with hemicellulose and lignin to form the macrofibrils (25–30 nm). Lignin is the "cementing agent/matrix component of wood". Hemicellulose is the "bonding agent between lignin and cellulose" (Toumpanaki et al., 2021). For what is concerning the use of AFM, Toumpanaki and coworkers mention the investigation by Fahlén and Salmén, 2005, about the pore size and distribution in the fiber wall obtained by means of atomic force microscopy (AFM) and image analysis.

AFM is given as a suitable tool for the study of fiber microstructures by Geoffrey Daniel, 2016, in his detailed description of microscope techniques available for "understanding wood cell structure". The Figure 15.1 of Daniel's work is proposing a simplified overview of microscopy techniques, each of them hierarchically related to wood structures. The fiber ultrastructure can be investigated by means of FE-Cryo-SEM (Cryo Field Emission Scanning Electron Microscopy, 5-10 nm), FE-SEM (Field Emission Scanning Electron Microscopy, > 1.5 nm) and TEM (transmission electron microscopy, > 0.2 nm). Actually, the cryo-SEM has been proved by Lyczakowski et al., 2019, as a useful method to investigate hardwood and softwood cell walls at their native nanoscale architecture. Lyczakowski and coworkers confirmed that cell wall macrofibrils, which have a cylindrical form with diameters exceeding 10 nm, are common in the samples obtained from native hardwood and softwood.

Cell walls

Nopens et al., 2020, have considered the mesopores in the wood cell wall at dry and wet conditions, for the question concerning how water is present and stored in the wood structure. In cellulose, water has been distinguished as "free water, freezing-bound water and non-freezing bound water" (Nopens et al., 2020, Nakamura et al., 1981), but it is also assumed that "only non-freezing bound water is present in the cell wall" (Nopens et al., 2020, Engelund et al., 2013, Willems, 2016). Moreover, it is also generally assumed that the absorption of water induces a sort of porosity within the cell wall.

After remembering the IUPAC classification of the pore size, Nopens and coworkers note that the size of the pores has a role in the freezing and melting behavior in meso- and macropores. "With smaller pore size, *freezing* temperature is shifted to lower temperatures (Table 1)", as determined by means of the cryoporometry. Table 1 of the article by Nopens et al. is giving the "isothermal step *heating* program with related pore size distribution based on the Gibbs-Thomsen-Equation for cylindrical pores" [actually, Gibbs-Thomson-equation]. The method has a resolution boundary of 2–3 nm pore size, because no melting of water can be observed below this size. The reference by Nopens and coworkers is Park et al., 2006. Park and coworkers give the relation between the pore diameter D and the *depressed melting temperature* $T(D)$, in the form of the Gibbs–Thomson equation:

$$\Delta T = T_0 - T(D) = -\frac{4 T_0 \gamma_{ls}}{D \rho H_f} \cos\phi \qquad (1)$$

In (1), T_0 is the melting temperature of water (273.15 K), γ_{ls} is the surface energy at ice-water interface (12.1 mJ/m^2), ρ, H_f are density and bulk enthalpy of fusion (specific heat of fusion) of freezing bound water, assumed to be equal to that of unbounded water (1000 kg/m^3 , 334 J/g). D is the diameter of the pore. ΔT is the melting temperature depression, and the water in a *smaller* pore has a *larger* melting temperature depression. Usually, angle ϕ is assumed to be near 180° in cylindrical pores.

In dimensions, (1) gives: $\left[\frac{k_B \Delta T}{k_B T_0}\right]=\left[\frac{\gamma_{ls}}{D\,\rho\, H_f}\right]=\left[\frac{energy\times L^{-2}}{L\times M\times L^{-3}\times energy\times M^{-1}}\right]=\left[\frac{energy}{energy}\right]$, where k_B is the Boltzmann constant, and *M, L* are the dimensions of mass and length.

Let us also remember the expression of the Gibbs-Thomson effect given by Jackson and McKenna, 1990, of the melting point depression for a small spherical crystal (size *d*) in its own liquid in the form:

$$\Delta T = T_0 - T(d) = \frac{4 T_0 \gamma_{ls}}{d\,\rho\, H_f} \qquad (2)$$

It is assumed an isotropic surface energy at solid-liquid interface and that the crystal side is sufficiently large that the material retains its bulk properties for density and specific heat.

Jackson and McKenna investigated the phase transition temperatures and heats of fusion for nonpolar organic materials (cis- and trans-decalin, cyclohexane, benzene, chlorobenzene, naphthalene, heptane) confined in controlled pore glasses. The pore diameter *D* was in the range of 4–73 nm. As for the previously studies of inorganic materials, the melting point *T*(*D*) decreased with decreasing pore diameter. Also a reduction in the bulk enthalpy of fusion was measured.

Considering again the work by Nopens and coworkers on wood, the researchers conclude that their "results strongly support the assumption that mesopores are *not present within the dry or wet wood cell wall*. This is in contradiction to existing literature were mesopores are show for wood" with different measurements techniques (see references mentioned by Nopens et al.). In fact, "pore sizes of the wood are expected to be in the mesoporous range", and Nopens and coworkers mentions Kojiro et al., 2010, who considered the micropores and mesopores in the cell wall of dry wood, and also Gao et al., 2017, Sawabe et al., 1973, Grigsby et al., 2013.

In a very recent work, Zhong and Ma, 2022, are considering the same subject. They propose an approach to study the pore size distribution in the wood cell wall, based on data provided by differential scanning calorimetry (DSC) thermoporometry, in the framework of a continuous method. "The pore size distribution (PSD) of cell wall is crucial for the wood", and can be analyzed by means of "the heat absorption of cell wall water upon melting" (Zhong & Ma, 2022). Chinese fir was investigated. The results obtained by Zhong and Ma showed that cell wall pores above 20 nm hardly existed. For a detailed discussion about the thermoporometry by means of the differential scanning calorimetry, see please Landry, 2005.

The method for the simultaneous determination of shape and size of pores was proposed in 1977 by Brun et al. Landry is mentioning the fact that "no general consensus for DSC temperature programs, as experimental conditions are often dictated by many variables". The variable are regarding "the characteristics of the porous solid, the solidification temperature of pore-filling liquid, the sample size, the instrument capabilities, and most often, the analyst preferences" (Landry, 2005).

Zhong and Ma conclude that most wood cell wall pores had a diameter less than 10 nm. As "the pore diameter increased, the differential pore volume decreased sharply". The continuous DSC thermoporometry method has been proposed by Zhong and Ma as more reliable than discontinuous methods earlier reported. They stress that "the quantitative analysis of the two methods [continuous and discontinuous] was quite different. Specifically, the pore volume calculated by the continuous method was 9.4–52.4 times larger than that derived by the discontinuous method" (Zhong & Ma, 2022).

Gibbs composite-system thermodynamics

As we can find told by Michael R. Landry, 2005, the thermoporometry is a measurement method of the pore size, obtained by means of the "melting or freezing point *depression* of a liquid confined in a pore". The depression is due to the "contribution of surface curvature to the phase-transition free energy". In the article by Landry, a specific section is discussing the "heating versus cooling experiments", where it is stressed that it is important to distinguish the two measures, in heating and cooling, In literature, we can find both mentioned and evaluated the melting and freezing point depression of temperatures.

Eq. 12 in the article by Landry is giving the relationship between the temperature depression ΔT and the pore size d is given as (note the approximation):

$$\Delta T \approx \frac{4 T_0 \gamma_{ls}}{d \rho_l H_f} \cos\phi \qquad (3)$$

The density is that of the liquid mass. Note that the sign of the temperature shift depends on the value of angle ϕ . Please consider the derivation of this equation in the Appendix of Landry's work.

Equation (3) is "*analogous* to the Gibbs–Thompson equation", the equation regarding the melting point depression for "small crystalline solids" (Landry, 2005). It is also noted that literature considers as usual the existence of a layer of non-freezable liquid "along the walls of a porous material". As given by Landry, the melting point shift for a mesoconfined solid phase can be obtained from the Gibbs surface thermodynamics. In 2020, Janet Elliott has also discussed this thermodynamics required by composite materials, remembering that it is based on the work by J. W. Gibbs, “On the Equilibrium of Heterogeneous Substances”, published in two parts in 1876 and 1878 respectively. Its applications are mainly in the fields of biotechnology and nanoscience, including the systems with interfaces, curved interfaces and multicomponent phases (Elliott, 2020).

In the SSPCMs, the melting point shift can be relevant and detected by differential scanning calorimetry. Also in the case of a micro-encapsulation of the phase change material the depression is observed. Let us remember that microencapsulated PCMs, or MicroPCMs, are consisting of 3 to 100 micron size particles made of a PCM core in a polymer shell (Dolez & Vu-Khanh, 2009). Cao et al. (2014), for instance, have microencapsulated the palmitic acid (PA) with TiO_2 shell. The researchers observe that the phase change features of this MicroPCM are close to those of the PA, but the temperatures of melting and solidification are lower than those of PA. The Gibbs–Thomson effect and the related *temperature shift* is mentioned as the reason of this behavior. The *sign* of the *temperature shift* is related to the *difference* of solid/wall interfacial energy and the liquid/wall interfacial energy.

For confined PA in MicroPCMs, we have a temperature depression, "inversely proportional to the pore size, as given by the Gibbs–Thomson equation" (Cao et al. are mentioning Warnock et al., 1986, and Evans, 1990). The Table 2 in Cao et al., 2014, is giving the following DSC data.

Sample	Melting Temperature (°C)	Solidifying Temperature (°C)
PA	62.6	60.5
Micro-PCM-1	61.7	56.7
Micro-PCM-2	60.7	44.2
Micro-PCM-3	60.7	52.8

In Sparavigna, 2022, we have considered the biochar for SSPCMs. The Gibbs-Thomson equation is rarely mentioned; we can find it in Webber et al., 2013, and Wong et al., 2019. As noted by Bordoloi et al., 2022, the melting point shift observed in biochar-based SSPCMs is caused by several reasons. Among those mentioned we can find "the enhancement of surface to volume ratio in the composite material compared to bulk original PCM", that is the effect of which are discussing now. There are also a "weak interaction of PCM and the inner surfaces of the supporting matrix", and an "increase irregularities in PCM crystals due to pores" and consequent increase of lattice defect.

Bikbulatova et al., 2018, considered the water retention behavior in biochar. The researchers produced biochar from peanut and palm kernel shells and observed that "Water holding capacity and water adsorption rate showed a direct correlation with micropore volume of biochar, suggesting that physical structure of biochar played a key role during interaction with water" (Bikbulatova et al., 2018). The water was considered as freezable free water (FFW) and freezable bound water (FBW). "The phase transition temperature of freezable bound water correlated well with pore size distribution of bio-chars" (Bikbulatova et al., 2018), but the presence of non-freezable (NFW) water in biochar has been also confirmed. About the Gibbs-Thomson equation, Bikbulatova and coworkers are mentioning Findenegg et al., 2008, who considered the water freezing and melting in silica nanopores.

Findenegg and coworkers consider Gibbs-Thomson in the form:

$$T_p(R) - T_0 = -\frac{C}{R} \quad \text{with } C = \frac{2T_0 v(\gamma_{WS} - \gamma_{WL})}{\Delta h_{SL}} \qquad (4)$$

Quantities γ_{WS}, γ_{WL} are the surface free energies per unit area of two interfaces, wall/solid and wall/liquid. Δh_{SL} is the enthalpy and v the volume of the liquid or solid phase, "depending on which has the lower surface free energy against the wall" (Findenegg et al., 2008). The equation can be rewritten by means of the Young's equation:

$$\gamma_{WS} - \gamma_{WL} = \gamma_{SL} \cos\phi \qquad (5)$$

γ_{SL} is the interfacial tension of ice/water, ϕ represents the contact angle formed by the ice/water interface with the wall (Findenegg et al., 2008). Eq.4 gives a *melting temperature in pores which can be depressed or elevated, depending on the difference between the surface energies*. As stressed by Findenegg and coworkers, "in most cases the former situation $(\gamma_{WS} - \gamma_{WL} > 0)$ prevails, since liquids can adapt to rough pore walls better than crystalline solids". In the article by Findenegg et al. we can find also two wetting scenarios: the partial wetting case and the complete wetting case. In the case of the complete wetting, due to a strong feeling of the pore wall for liquid, "a thin liquid-like layer starts to form at the solid/wall interface at a temperature well below" the pore melting

temperature. "The existence of such a premelted layer at the pore walls is not accounted for in the original Gibbs–Thomson relation" (Findenegg et al., 2008).

Using mesoporous silica materials MCM-41 and SBA-15 of well-known pore radius R, Findenegg and coworkers are the fitting data with the curve:

$$\Delta T_p(R) = \frac{C}{R-t} \qquad (6)$$

Forcing a fit with $t = 0$ is not possible for pore radii $R < 2$ nm. Therefore, it is suggesting that the pores have an effective radius $R_S = R-t$, where t is the thickness of a liquid-like layer. MCM-41 and SBA-15 mesoporous silicas with lauric acid (LA) have been considered in work by Mitran et al., 2015. Mitran and coworkers, "Taking into account that no strong hydrogen bonding between the carboxyl groups of LA and the silica support are formed", are considering the Gibbs−Thomson equation to evaluate the melting point depression.

Besides the interaction between PCM and the wall of the pores, there is also another factor to consider and it is the complete or partial filling of the pores. Then the experimental study of the Gibbs-Thomson effect in the case of wood or biochar is not easy but possible, and it could provide information about the pores in them.

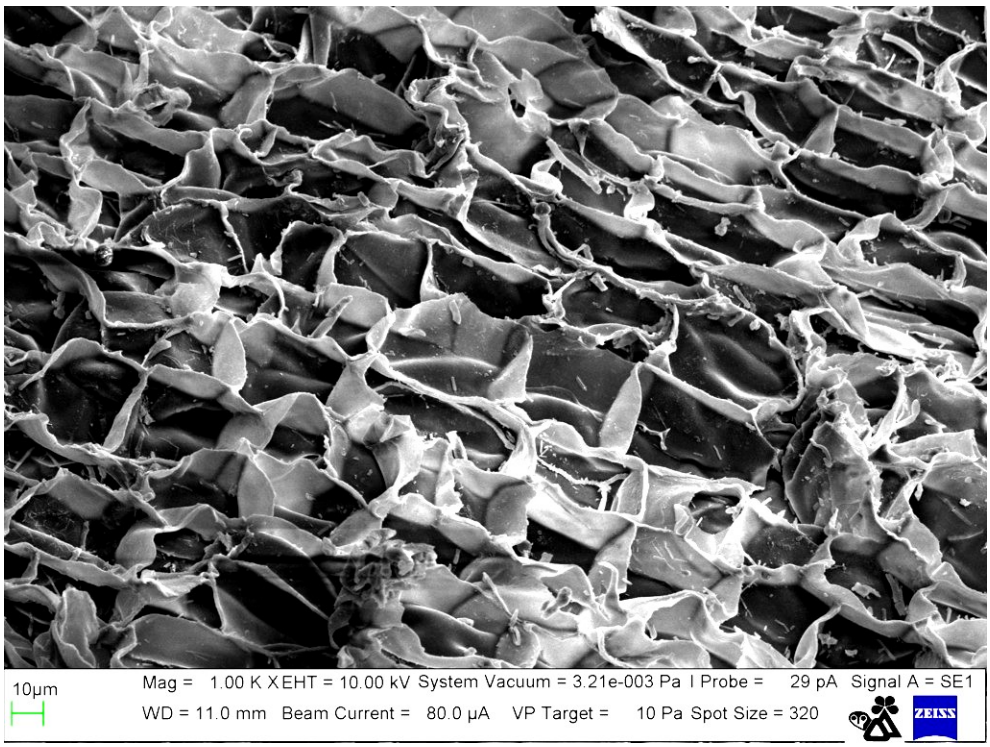

Figure 4 - Scanning electron microscope image of cork. Image courtesy of the author Nicola Angeli, MUSE, Science Museum of Trento, in the framework of the cooperation Wikimedia Italia - MUSE. License Attribution-ShareAlike 3.0 Unported (CC BY-SA 3.0) as declared at https://en.wikipedia.org/wiki/Cork_(material)#/media/File:Cork_1000x_-_SEM_MUSE.tif (https://archive.vn/rgcve)

Core and bark

Let us start the discussion about the wood-based composite PCMs.

Nam et al., 2022, are proposing an experimental work about the potential of wood for application in the thermal energy storage. They investigated the thermal characteristics of wood, which are depending on its hierarchical structure. As noted by Nam and coworkers, wood is made of a hard core and an outer bark. Core and bark have been impregnated by PCMs. The difference in their structural and chemical compositions - the researchers observed - has a significant influence on PCM impregnation. The role of the hierarchical structures in core and bark was analyzed referring to the thermal performance of the shape-stabilized PCMs (SSPCMs).

Cork is "a part of the harvested bark", considered as a waste byproduct of wood industry (Nam et al., 2022). Cork has a honeycomb structure containing large pores of approximately 27 μm (Wang et al., 2021). Its chemical composition is suberin (~50 wt.%), lignin (15-30 wt.%), polysaccharides (6-25 wt. %), and other extracts. The features of cork are: "impermeability, durability, heat and sound insulation, and shock absorption" (Nam et al., 2022).

Nam and coworkers report that the integration of PCMs in the porous structure of wood has been already considered. Among the researches mentioned by Nam et al., we can find the work by Saavedra et al., 2021, who impregnated the wood of the Pinus radiata tree of n-octadecane PCM and measured the mechanical properties of it. The thermal characterization has been previously made by Fuentes-Sepúlveda et al., 2020. The observed minimum and maximum enthalpies are of 36 J/g and 122 J/g, according to the orientation of the wood. Nam et al. (2022) used balsa wood and cork, determining the chemical bonds which were formed between wood and PCM during the preparation of an SSPCM. The features of the composites were evaluated to determine the use for building materials. As stressed by the researchers, the phase change temperature suitable for applications in buildings is approximately 27°C-35°C (Jeon et al., 2019), and the n-octadecane as PCM is a proper choice. When the PCM has been successfully inserted into the pores of balsa and cork, it is observed that wood/PCM composites have a hydrophobicity which is stronger than that of the pristine material. Wood with its porous structure has a natural large water absorption. If pores are filled by the PCM, the wood cells reduce their water absorption. The microstructural changes due to the presence of PCM can be observed through SEM analysis. For what concerns the latent heat of SSPCMs, balsa-based and cork-based composites have different performances, about 50 J/g for balsa-PCM and about 131 J/g for cork/PCM (Nam et al., 2022). It means that cork seems being better for thermal energy storage.

In the Table 6 of the article by Nam et al., we can find temperatures and latent heats. Here the results for the PCM (n-octadecane) and the SSPCMs in balsa and cork.

Specimen	Melting T (°C)	Freezing T (°C)	Melting (J/g)	Freezing (J/g)
n-octadecane	29.765	23.171	180.73	184.83
Balsa-n-octadecane	26.467	23.747	49.66	49.63
Cork-n-octadecane	27.720	23.397	131.20	131.22

Here we can find a depressed melting temperature in balsa and cork. The freezing temperature is slightly increased.

Delignified wood

Vitas et al., 2019, stress that the outstanding structures of wood can be used to fabricate hierarchical and functional materials. The researchers observed that, with delignification[1] treatments, density and chemistry of wood can be altered. In particular an enhanced porosity is observed, suitable for the fabrication of novel hybrid materials. In the case of thermal energy storage, Liu et al., 2021, proposed composites based on the delignified balsa wood.

Liu and coworkers prepared the composites through a vacuum impregnation method using chemically treated wood (CTW) and myristic acid (MA), paraffin (PW) and polyethylene glycol (PEG) as PCMs. After the chemical treatment, lignin and hemicellulose in the wood are removed, so that the density of wood is reduced and more PCM absorbed. A latent heat as high as 181.9 J/g was observed.

Sample	Melting Temperature (°C)	Crystallization Temperature (°C)
MA	56.1	49.7
MA/CTW-2	55.7	49.6
PW	60.3	56.8
PW/CTW-2	60.3	56.9
PEG	56.3	37.7
PEG/CTW-2	55.8	33.8

The weight percent of PCM in CTW-2 is 83.9%.

The balsa wood was prepared as follow. The natural wood blocks were immersed in 2.5 mol/L NaOH and 0.4 mol/L Na_2SO_3 aqueous solution, heating the biomass under reflux. Heating under reflux is a procedure which is heating the reactants for a specific amount of time, while vapors condense back to liquid form. The balsa samples were taken out after 4 h, 8 h and 12 h, and washed carefully. The samples were "delignified wood samples", which were freeze-dried for 12 h. The samples had different degrees of lignin removal.

Chemically, the lignin is a polymer made by cross-linking phenolic precursors (Lebo et al., 2001). This polymer is giving to the wood cell walls stability and protection against external factors. The delignification of wood is creating an environment where free hydroxyl groups appear as potential functional sites (hydroxyl groups are relevant for the water sorption, White & Eyring, 1947, Berthold et al., 1996). The delignified wood turns into an environment sensitive to moisture or water, due to the removal of the hydrophobic lignin from the cell wall. Moreover, the cellular structure turns to be open (Kumar et al., 2021). As stressed by Kumar and coworkers the estimation of mesoporosity and moisture behavior of the delignified wood is fundamental to establish the functional ability of this wood material.

1 Delignification is the process of extracting lignin from wood, and can be performed in a variety of manners. Its aim is that of disintegrating the ligno-cellulosic scaffold to obtain the cellulose fibers (Wool, 2011). The delignification processes can be subdivided into chemical and solvent processes.

About the delignified wood and its application, a review is given by the mentioned reference (Kumar et al., 2021). Kumar and coworkers observe that the cellulose structure can be used as a natural scaffold for several functional applications. The first and second part of the discussion by Kumar et al. is regarding wood structure, wood chemistry, lignin biosynthesis and different delignification methods. The third part of the review is devoted to applications. In the review, delignified wood-based composite PCMs are discussed too. The researchers remember that the greatest disadvantage of PCMs is their shape-instability (leakage) during the transition. "DW [delignified wood] could be a potential candidate for a new PCM due to its extremely high hygroscopic behavior" (Kumar et al., 2021). Therefore the hierarchical cellulose structure of DW can provide stability to PCMs.

Ma et al., 2019, investigated DW (cedar wood slices) in composites with different weight percentages of capric–palmitic acid eutectic mixtures (CA–PA) as PCM. The mixture was vacuum impregnated into natural and DW. The CA–PA forms hydrogen bonds with the OH groups present in the delignified wood. As illustrated by the Figure 22 in Kumar et al., 2021, the SEM imagery shows that CA-PA is filling the pores with a clear difference between DW and natural wood. After the process of delignification, "the cell wall became more porous with a wider cell lumen area. Delignification opened the cellular structure of natural wood", tell Kumar and coworkers. In the DW, there is a "sufficient passage for molten CA–PA penetration and homogeneous deposition in the cell wall structures" (Kumar et al., 2021). Heat of fusion of CA–PA and melting temperature are about 153 J/g and 23 °C, respectively (in cooling, 151 J/g and 14 °C). The DW/CA–PA composite shows a similar behavior with values of about 94 and 91 J/ g in melting and cooling respectively (Kumar et al., 2021). The latent heat is reduced, however DW could be suitable for various applications of PCMs in energy systems and for thermal insulation of buildings, as stressed by Kumar and coworkers. Incorporating PCMs into building compartments is also useful for a passive cyclical release and absorption of heat, in order to reduce the energy consumption for heating and cooling (Jamekhorshid et al., 2017).

In the review, it is also mentioned the "*magnetic* wood-based composite PCM" obtained by the delignified balsa wood (Yang et al., 2019). Magnetic Fe_3O_4 nanoparticles were mixed with melted 1-tetradecanol and balsa DW vacuum impregnated. According to Yang and coworkers, "the addition of Fe_3O_4 nanoparticles provides an excellent magnetic property and improves the solar-to-thermal conversion efficiency of the composite". Due to the magnetothermal effect, the "magnetic wood-based composite phase change materials can be heated under an alternating magnetic field" (Yang et al., 2019). The exhibited latent heat is of 179 J/g.

Magnetic Fe_3O_4 is present in another study too. A magnetic Fe_3O_4/ZIF-67/DW aerogel has been proposed by Xu e tal., 2019, with efficient microwave absorption properties. The Fe_3O_4/ZIF-67 dodecahedrons served as the absorbing agents. Kumar and coworkers are also mentioning the work by Wang et al., (2020), that prepared a DW and microPCM emulsion-based composite PCM. The DW was impregnated via vacuum infusion.

Transparent wood

Before continuing the discussion about the lignin removal, let us mention an important application of the process. It is the production of "transparent wood".

Li et al., 2016, obtained an optically transparent wood, transmittance 85% and haze 71%, using a nanoporous cellulosic template. The template was obtained by removing the lignin, which is the light-absorbing component. The pores of the delignified wood were impregnated with methyl methacrylate (MMA), possessing a matched refractive index. The result was a lightweight strong transparent wood for windows. As told by Li and coworkers, the light scattering happens at the interfaces between cell walls and air. Moreover, a light absorption is observed due to wood biopolymers. A strong absorption, 80-95% of light, is due to lignin. Therefore the first step to obtain a transparent wood is the removal of

lignin. After the process of delignification, the wood turns into a white cellulose-rich template, where the honeycomb-like structure of the wood and the nanoscale cell wall organization remain well-preserved. Li and coworkers further investigated the nanostructure of the template, by means of high-resolution SEM images (see the images in the work by Li et al., 2016). "At very small scale, Figure 2b indicates that there is also *nanoscale porosity resulting from lignin removal*". The specific surface area passed from a value of 1.2 m^2/g of the original wood to the value of 19.8 m^2/g in delignified wood. "The increased surface area is beneficial" for the impregnation of the porous template.

Literature on transparent wood is provided, among many others, by the articles of Li et al., 2018, Bisht et al., 2021, Muthoka et al. 2021, Zhu et al., 2022.

Montanari et al., 2019, have proposed the transparent wood for the thermal energy storage too. According to Montanari and coworkers, the composite PCMs are "under rapid development". Again, we can find assumed the mesoporous frameworks as "ideal carriers" the phase-change materials, being able to provide shape stability over the thermal cycles. The researchers have produced a composite PCMs based on transparent wood for the encapsulation of polyethylene glycol PEG. The delignified wood has been fully characterized, even in its nano- and mesoscale structures. The composite has a latent heat of about 76 J/g, combined with a "switchable optical transparency". The support of PCM is a mesoporous DW template, impregnated by a PEG/MMA blend. Actually, the melting temperature of the transparent-wood composite is larger than that of PEG (38.3 instead of 37.8 degrees). The analysis of the wood template composite morphology shows that "a PEG-rich phase was present *in the wood cell wall*, in the form of 100−200 nm mesoscale domains" (Montanari et al., 2019).

Singh et al., 2022, are also talking of "porous wood scaffolds" (PWS) that has emerged from the "traditional delignification or bleaching method", obtaining the creation of "nanoscale pores within cell walls and microscale pores within cell wall corners and middle lamella" (Fu et al., 2017). The mechanical features of the PWSs is lower than that of wood, but the impregnation of polymers can improve them. The impregnation of cell walls and lumen spaces, as for instance in the transparent wood, allows to add the structural performance to the functional character of the added material. But, a "remaining challenge for the functional transparent wood", according to Singh and coworkers, 2022, is that of obtaining a "fully sustainable" composite made of "entirely bio-based components and polymers". And in fact, as mentioned by Singh and coworkers, Montanari et al., 2021, have prepared a "fully bio-based transparent wood biocomposite" using limonene acrylate monomer and PWS. The monomer has a chemical structure which enables the diffusion into the cell wall. The monomer than polymerizes and the polymer phase has the refractive index matched to that of the wood substrate. The biocomposite has an optical transmittance of 90% for a thickness of 1.2 mm, a haze of 30%, and high mechanical performance.

Lignin removal and mesopores

In the review by Kumar et al., 2021, it is told that Liang et al., 2020, evaluated the effects of the lignin removal on the mesoporous structure of poplar cell walls. The researchers performed nitrogen absorption experiments so that to evaluate specific surface area, pore volume and mesoporous distribution. The methods of evaluation were based on BET (Brunauer–Emmett–Teller) and BJH (Barrett–Joyner–Halena) models. The experimental results show that the pore size distribution is influenced by the different delignification stages. The pristine wood had two pore size separated distributions in the ranges of 10–50 nm (81%) and >50 nm (19%). After the 22% of delignification, it was observed that about the 64% of the pores was in the range about 1.97–2 nm. It is the removal of lignin which is promoting the formation of a large number of mesopores.

About the role of mesoporous structure in biochar-based SSPCMs we discussed previously (Sparavigna, 2022). For biochar, macropores are good for the diffusion of substances, mesopores are

channels for mass transfer and the micropores are trapping spaces for molecules, as told by Leng et al., 2021, and Chen et al., 2017. Bordoloi et al., 2022, stress that the mesoporous structure of biochar "is highly appreciated as scaffold material", whereas the microporous structure is "affecting in a negative manner the PCM thermal storage capacity". In the micropores, the molecules of the PCM are anchored to the pore walls and therefore not free to move to be effective for phase transition. For what concerns the macroporous structure, it is providing "the less capillary force". The researchers noted that the presence in biochar of active hydroxyl groups is enhancing the sorption capability of organic phase-change materials (Bordoloi et al., 2022).

Also for wood, the role of micro-, meso- and macropores has been considered, in particular regarding the role of the lignin removal, as we have previously seen. Meng et al., 2020, consider the mesoporous balsa after a selective removal of lignin. Meng and coworkers observed that delignification allows the development of mesopores and also an increase in the fluid permeability. In this manner, the wood becomes a system suitable to support PCM. Meng and coworkers used polyethylene glycol (PEG). They obtained a "form-stable PCM system (FPCM)" at temperatures above the melting transition temperature of PEG. The "encapsulation" was as high as 83.5%, latent heat of 134 J/g, with supercooling (12 °C). These results have been explained as coming from "the affinity between the unidirectional mesoporous structure and the PCM polymer, involving capillary forces and hydrogen bonding" (Meng et al., 2020). In the Table 1 of the article by Meng and coworkers we can find the transition temperatures.

Sample	Melting Temperature (°C)	Crystallization Temperature (°C)
PEG	43.6	26.9
W+P	39.8	28.6
W-L+P	40.0	27.7
W-L,H+P	40.9	27.2

In the Table we can find wood (W), delignified wood (W-L), delignified wood after removal of hemicelluloses (W-L,H), as well as after PEG loading ((W + P), (W–L + P), (W–L,H + P)).

In their work, Meng and coworkers are mentioning the research by Ma et al., 2019, observing that the near complete removal of hemicellulose and lignin by means of a $NaOH/Na_2SO_3$ treatment is facilitating the presence of a high porosity and therefore a suitable uptake of PCM. But. as observed by Kumar et al., the chemical treatment is degrading the structure of the cell wall. The mechanical performance of the delignified wood is reduced and this is producing leakage as consequence of loading. A selective removal of lignin and hemicellulose is therefore preferred to avoid the collapse of the scaffold under load.

Let us add also the work by Tian et al., 2022, that produced hierarchical porous biochar to encapsulate paraffin wax. The researchers removed lignin and hydrolyzed cellulose, so that the "macropore channels of reed stems were made to be connected via rich micropores on the carbon wall during high-temperature carbonization process". By loading this biochar with paraffin wax, a SSPCM has been obtained with high loading rate of about 93.5 wt%) and energy storage capacity of 141.47 J/g. Average pore sizes are raging from 1.85 nm to 2.55 nm.

Tian and coworkers consider carbonized samples. The samples with both delignified and enzymatical treatments are labeled as ER-x. The delignified reed stem samples without enzymatical treatment are denoted as DR-x. The "x" is the pyrolysis temperature (600, 700 and 800 °C). PW is the paraffin wax.

Sample	Melting Temperature (°C)	Solidification Temperature (°C)
PW	62.54	41.85
PW/ER-600	67.79	37.18
PW/DR-600	63.08	41.08
PW/ER-700	68.67	36.29
PW/DR-700	66.57	36.35
PW/ER-800	68.59	35.99
PW/DR-800	68.03	35.76

In the Tian and coworkers' article, the "melting and solidifying DSC curves of PW, PW/DR-600, PW/DR-700, PW/DR-800, PW/ER-600, PW/ER-700 and PW/ER-800 are displayed in Figs. 7a-b".

The researchers observe that samples have similar DSC curves. "However, as summarized in Table ... slightly higher melting temperature" of the composites than that of the paraffin wax was measured. Tian and coworkers attribute this fact to the "impeded thermal diffusion movement of PW crystals" inside the porous biochar, "because of the strong physical adsorption of PW through capillary interactions and interfacial tension" (Tian et al., 2022).

And here we can repeat Findenegg and coworkers' words: a melting temperature in pores can be "depressed or elevated, depending on the difference between the surface energies." In most cases we have a depression, "since liquids can adapt to rough pore walls better than crystalline solids". In the case of the biochar produced by Tian and coworkers we have an elevation.

Biochar of delignified wood

Since we have mentioned the biochar, let us consider the recent work by Dong et al., 2022, about biochar of delignified wood. Dong and coworkers consider the use of biochar as a facile and cost-efficient method to remove chromium VI from wastewater through adsorption. In the article published in 2022 the researchers combine delignification with a subsequent carbonization, followed by a KOH activation to obtain a biochar from waste poplar sawdust. Due to the porous structure provoked by delignification, the "*activated carbonized delignified wood*" (ACDW) possesses a high specific surface area of 970.52 $m^{2/}g$, in the framework of meso- and micropores with oxygen-containing functional groups. As stressed by Dong and coworkers, "ACDW delivers a remarkable adsorption capacity of 294.86 mg/g in maximum, which is significantly superior to that of unmodified counterparts and other reported biochars". The proposed adsorption mechanism is a combination of "capillary force, electrostatic attraction, chemical complexation, and reduction action" (Dong et al., 2022), which is capturing Cr(VI). The biochar which has been modified by KOH, is rich of functional

groups in the form of −COOH, −OH, and O═CH–, suitable to promote electrostatic interactions useful in the Cr(VI) removal.

First, it is performed the delignification which is modifying the cell walls into a multilayer structure with aligned cellulose fibers. The subsequent carbonization maintains the layered structure but it is also strongly increasing the porosity. "Further KOH activation" of the carbonized delignified wood, "optimizes the porous architecture and surface activity, leading to numerous meso- and micropores as well as rich oxygen-containing functional groups" (Dong et al., 2022). The carbonized wood (CW) and the carbonized delignified wood (CDW) display an adsorption type II isotherm, that, according to IUPAC classification is characterizing a typical mesoporous material. The activated CDW has an isotherm which is related to increasing micro-porosity.

Wooden cellulose and bacterial cellulose have been prepared by Yin et al., 2022. The composites were converted into carbon monoliths with hierarchically porous structure (CBC/CCW) by carbonization. The presence of both wooden and bacterial cellulose produces a scaffold with hierachically organized meso- and macropores.

Wood-flour

Cheng and Feng, 2020, produced SSPCMs based on delignified wood flour, to be used in the thermal management of buildings. The wood flour was delignified and impregnated with myristyl alcohol. The researchers observed that the wood micro-channel structure is maintained, and "unblocked" in the delignified wood flour, and this means that we can accommodate and maintain the PCMs in it. What is interesting in the work by Cheng and Feng is the fabrication of composite boards by bonding the SSPCM in the urea–formaldehyde resin. The resin is important also for the shape stabilization. In this manner, the resin improved both the thermal storage capacity and the mechanical performance of the composites.

Liang et al., 2018, worked for the fabrication of fatty acid/wood-flour composites as SSPCMs. Wood-flour, WF, has "low density, high porosity, high absorption capability, inertness and cheapness" and therefore it is a "good candidates as supporting materials for applications in buildings" (Liang et al., 2018). The structure of this flour is composed by cellulose fibers in a matrix of lignin, hemicellulose and cellulose, and this framework contains many hydroxyl groups; consequently, "organic PCMs can be incorporated into WF by hydrogen-bond interaction, capillary force and surface tension force to prevent the leakage during the phase transition process", this is told by Liang et al., mentioning Ma et al. 2018.

Ma and coworkers prepared a modified porous wood flour to be the support the lauric-myristic acid eutectic mixture (LA-MA) as PCM. The researchers investigated the effect of alkali (NaOH), cetyltrimethylammonium bromide (CTAB), and complex salts (CS) on the WF pore size.

The experimental results are given in the Table II of the article by Ma et al., 2018. We can find that the average pore diameter (nm) was: 8.73 (WF), 13.34 (NaOH-WF), 10.71 (CTAB-WF), 16.54 (CS-WF). *The experimental results indicated that the average pore diameter after impregnation was decreased to 5.85, 8.29, 6.78, and 6.32 nm, respectively*. When the eutectic mixture is incorporated into the pores, the pore diameter decreases. Ma and coworkers noted that the maximum impregnation ratio occurred for the CS-WF/eutectic, "because its average pore diameter decreased approximately 10 nm".

In the following table, the results proposed by Ma et al. in their Table 3, about the temperature transitions are given for the eutectic mixture and the composites.

Sample	Melting Temperature (°C)	Solidification Temperature (°C)
LA-MA	34.6	33.1
WF/LA-MA	33.1	32.6
NaOH-WF/LA-MA	33.5	32.3
CTAB-WF/LA-MA	33.9	32.6
CS-WF/LA-MA	33.1	32.9

As told by Ma and coworkers, "compared to the values of the pure LA-MA eutectic mixture, the melting temperature " of the composites "changed slightly and the latent heat values decreased due to the confinement of the LA-MA eutectic mixture's molecules in the pores" of the supporting material.

Let us stress the result obtained by the researchers: the average pore diameter after impregnation was decreased. This is an important fact to consider in the case that we want to link the melting temperature shift to the pore size.

Liang et al., 2018, tell also that few previous studies considered the wood flour as supporting microencapsulated organic PCMs (Li et al., 2009, Guo et al., 2016, Barreneche et al., 2017). The wood flour can be used to obtain boards as structural material for building and furniture. The composites prepared by Liang and coworkers had been obtained from lauric acid, myristic acid, hexadecanoic acid and stearic acid impregnating wood flour. The phase change properties, the thermal energy storage mechanism, and the thermal stability of the fatty-acid-wood-floud composites had been investigated.

Wood and microencapsulation

In 2009, Li et al. used wood-flour with high-density polyethylene as supporting material of micro-encapsulated paraffin as latent heat storage material. Moreover, graphite was added to improve thermal conductivity. Actually, another drawback of composite PCMs is a generally poor thermal conductivity which is disturbing the process of the thermal conversion.

Jeong et al., 2012, evaluated the performance of a microencapsulated PCM, suitable for the wood-based flooring application. This kind of flooring is commonly used in residential buildings in Korea, and it can be considered for heat storage. To increase the heat storage of the wood, the PCM was used with adhesive. It disperses well in adhesive. Jeong and coworkers have tested the composite, confirming that it has suitable features as a thermal energy storage material.

Today several commercial microencapsulated paraffin-based PCMs exist and had been tested for different applications (Giro-Paloma, et al., 2016, Castellón et al., 2006). Composites of wood-plastic with microencapsulated phase change material have been considered by Jamekhorshid et al., 2017. The wood-plastic composites are materials which are used in the building interior parts but these composites have low energy storage capacity. This capacity is increased by means of PCMs in the form of microencapsulated PCMs. No leakage is observed in the phase change. Jamekhorshid and coworkers are also mentioning the commercially available DuPont™ Energain® wallboards, suitable for comparison of the prepared composites.

Thermochromic PCMs

Yang et al., 2018, prepared a composite PCM using the delignified poplar wood. Latent heat and phase change temperature (melting) were about 118 J/g and 34 °C respectively. The peculiarity of this composite is its reversible thermochromic property. The termochromic PCMs were prepared by mixtures of crystal violet lactone, bisphenol A and tetradecanol. When the tetradecanol is liquid, the composite is colorless, otherwise it is blue. Zhang et al., 2022b, who are proposing a review of composite PCMs based on biomass materials, tell that few studies are regarding the direct visualization of the phase change process of PCMs. The direct visualization can be achieved when a thermochromic material is inserted in the PCM. In the review we can find mentioned the work by Yang et al., 2018, and those by Heng et al., 2020, and Feng et al., 2020.

Regarding the work by Yang et al., 2018, let us add that the DSC results of pure 1-tetradecanol TD, thermochromic TC compound, TCPWs (pristine wood) compound and TDDWs, TCDWs (delignifed wood) compounds are presented in their Fig. 8 and Table 2. "The DSC curves show one endothermic peak on heating and two exothermic peaks on cooling" (Yang et al., 2018). The endothermic peak is given by the overlapping solid-solid and solid-liquid transitions. The two exothermic peaks are related to the liquid-solid transition and the solid-solid transition. In the following table, the results for TD and TDDWs are given.

Sample	Melting Temp. (°C)	Solidification Temp. (°C)	Solid-solid Trans. (°C)
TD	37.34	36.75	33.29
TDDWs	36.87	37.03	30.71

Heng and coworkers developed a thermochromic bamboo-based composite PCM with phase change at about 41 °C and latent heat of about 113 J/g. The proposed bamboo-based composite PCM has a reversible thermochromism and thermal properties, which are rendering it proper for applications in thermal insulation and temperature control in the form of interior decoration materials (Zhang et al., 2022b). Feng and coworkers use also delignified bamboo and a different thermochromic compound, so that this other bamboo-based reversible thermochromic composite PCM has different transition temperature at 40.5 °C and latent heat of about 115 J/g. For more detailed data, see please the works by Heng et coworkers and Feng and coworkers.

As stressed by Zhang et al., 2022b, "the research on biomass-based thermochromic composite PCMs is still in its infancy, with few reports at present".

Thermal stability

To conclude, it is necessary to remark the importance of the thermal stability for composite PCMs, because they may be subjected to degradation under the repetition of storage cycles. A material which is reliable for applications needs to be chemically, physically and thermally stable, after a large number of thermal cycles have been performed. Of course, this is especially important for latent heat and melting point after a repeated number of thermal cycles (Rathod, 2018). As for other composite PCMs, thermal stability is fundamental for the practical application value of the wood-based PCMs. It means that the wood-based PCM, heated up to the melting point, maintains its shape remaining confined in the pores without leakage, and this happens over several thermal cycles of the composite.

References

[1] Abdeali, G., Bahramian, A. R., & Abdollahi, M. (2020). Review on nanostructure supporting material strategies in shape-stabilized phase change materials. Journal of Energy Storage, 29, 101299.

[2] Akgün, M., Aydın, O., & Kaygusuz, K. (2007). Experimental study on melting/solidification characteristics of a paraffin as PCM. Energy Conversion and Management, 48(2), 669-678.

[3] Barreneche, C., Vecstaudza, J., Bajare, D., & Fernandez, A. I. (2017). PCM/wood composite to store thermal energy in passive building envelopes. In IOP Conference Series: Materials Science and Engineering, Vol. 251, No. 1, p. 012111. IOP Publishing.

[4] Bartoli, M., Giorcelli, M., Rosso, C., Rovere, M., Jagdale, P., & Tagliaferro, A. (2019). Influence of commercial biochar fillers on brittleness/ductility of epoxy resin composites. Applied Sciences, 9(15), 3109.

[5] Bartoli, M., Giorcelli, M., Jagdale, P., Rovere, M., & Tagliaferro, A. (2020). A review of non-soil biochar applications. Materials, 13(2), 261.

[6] Bartoli, M., Giorcelli, M., Jagdale, P., & Rovere, M. (2020). Towards traditional carbon fillers: biochar-based reinforced plastic. In Fillers. IntechOpen.

[7] Bartoli, M., Rosso, C., Giorcelli, M., Rovere, M., Jagdale, P., Tagliaferro, A., Chae, M., & Bressler, D.C. (2020). Effect of incorporation of microstructured carbonized cellulose on surface and mechanical properties of epoxy composites. Journal of Applied Polymer Science, 137(27), 48896.

[8] Bartoli, M., Arrigo, R., Malucelli, G., Tagliaferro, A., & Duraccio, D. (2022). Recent advances in biochar polymer composites. Polymers, 14(12), 2506.

[9] Bates, A., & Draper, K. (2019). Burn: using fire to cool the earth. Chelsea Green Publishing.

[10] Berthold, J., Rinaudo, M., & Salmeń, L. (1996). Association of water to polar groups; estimations by an adsorption model for ligno-cellulosic materials. Colloids and Surfaces A: Physicochemical and Engineering Aspects, 112, 117–129.

[11] Bikbulatova, S., Tahmasebi, A., Zhang, Z., Rish, S. K., & Yu, J. (2018). Understanding water retention behavior and mechanism in bio-char. Fuel Processing Technology, 169, 101-111.

[12] Binder, K. (1987). Theory of first-order phase transitions. Reports on progress in physics, 50(7), 783.

[13] Bisht, P., Pandey, K. K., & Barshilia, H. C. (2021). Photostable transparent wood composite functionalized with an UV-absorber. Polymer Degradation and Stability, 189, 109600.

[14] Blanchet, P., & Pepin, S. (2021). Trends in chemical wood surface improvements and modifications: a review of the last five years. Coatings, 11(12), 1514.

[15] Bordoloi, U., Das, D., Kashyap, D., Patwa, D., Bora, P., Muigai, H. H., & Kalita, P. (2022). Synthesis and comparative analysis of biochar based form-stable phase change materials for thermal management of buildings. Journal of Energy Storage, 55, 105801.

[16] Brassard, P., Godbout, S., Lévesque, V., Palacios, J. H., Raghavan, V., Ahmed, A., Hogue, R., Jeanne, T., & Verma, M. (2019). Biochar for soil amendment. In Char and carbon materials derived from biomass (pp. 109-146), Elsevier, 2019.

[17] Brun, M., Lallemand, A., Quinson, J. F., & Eyraud, C. (1977). A new method for the simultaneous determination of the size and shape of pores: the thermoporometry. Thermochimica acta, 21(1), 59-88.

[18] Cao, L., Tang, F., & Fang, G. (2014). Preparation and characteristics of microencapsulated palmitic acid with TiO2 shell as shape-stabilized thermal energy storage materials. Solar energy materials and solar cells, 123, 183-188.

[19] Castellón, C., Nogués, M., Roca, J., Medrano, M., & Cabeza, L. F. (2006). Microencapsulated phase change materials (PCM) for building applications. ECOSTOCK, New Jersey.

[20] Cheng, B. H., Tian, K., Zeng, R. J., & Jiang, H. (2017). Preparation of high performance supercapacitor materials by fast pyrolysis of corn gluten meal waste. Sustainable Energy & Fuels, 1(4), 891-898.

[21] Cheng, L., & Feng, J. (2020). Form-stable phase change materials based on delignified wood flour for thermal management of buildings. Composites Part A: Applied Science and Manufacturing, 129, 105690.

[22] Daniarta, S., Nemś, M., Kolasiński, P., & Pomorski, M. (2022). Sizing the Thermal Energy Storage Device Utilizing Phase Change Material (PCM) for Low-Temperature Organic Rankine Cycle Systems Employing Selected Hydrocarbons. Energies, 15(3), 956.

[23] Daniel, G. (2016). Microscope techniques for understanding wood cell structure and biodegradation. In Secondary xylem biology (pp. 309-343). Academic Press.

[24] Danish, A., Mosaberpanah, M. A., Salim, M. U., Ahmad, N., Ahmad, F., & Ahmad, A. (2021). Reusing biochar as a filler or cement replacement material in cementitious composites: A review. Construction and Building Materials, 300, 124295.

[25] Das, C., Tamrakar, S., Kiziltas, A., & Xie, X. (2021). Incorporation of biochar to improve mechanical, thermal and electrical properties of polymer composites. Polymers, 13(16), 2663.

[26] Dolez, P. I., & Vu-Khanh, T. (2009). Gloves for protection from cold weather. In Textiles for Cold Weather Apparel (pp. 374-398). Woodhead Publishing.

[27] Dong, H., Zhang, L., Shao, L., Wu, Z., Zhan, P., Zhou, X., & Chen, J. (2022). Versatile Strategy for the Preparation of Woody Biochar with Oxygen-Rich Groups and Enhanced Porosity for Highly Efficient Cr (VI) Removal. ACS Omega, 7(1), 863-874.

[28] Du, K., Calautit, J., Wang, Z., Wu, Y., & Liu, H. (2018). A review of the applications of phase change materials in cooling, heating and power generation in different temperature ranges. Applied energy, 220, 242-273.

[29] Elliott, J. A. (2020). Gibbsian surface thermodynamics. The Journal of Physical Chemistry B, 124(48), 10859-10878.

[30] Engelund, E. T., Thygesen, L. G., Svensson, S., & Hill, C. S. (2013). A critical discussion of the physics of wood–water interactions. Wood Science and Technology, 47, 141–161.

[31] Evans, R. (1990). Fluids adsorbed in narrow pores: phase equilibria and structure. Journal of Physics: Condensed Matter, 2(46), 8989.

[32] Fahlén, J., & Salmén, L. (2005). Pore and matrix distribution in the fiber wall revealed by atomic force microscopy and image analysis. Biomacromolecules, 6(1), 433-438.

[33] Fang, Q. R., Makal, T. A., Young, M. D., & Zhou, H. C. (2010). Recent advances in the study of mesoporous metal-organic frameworks. Comments on Inorganic Chemistry, 31(5-6), 165-195.

[34] Feng, N., Liang, Y., & Hu, D. (2020). Delignified bamboo as skeleton matrix for shape-stable phase change heat storage material with excellent reversible thermochromic response property. Journal of Energy Storage, 30, 101401.

[35] Findenegg, G. H., Jähnert, S., Akcakayiran, D., & Schreiber, A. (2008). Freezing and melting of water confined in silica nanopores. ChemPhysChem, 9(18), 2651-2659.

[36] Fu, Q., Medina, L., Li, Y., Carosio, F., Hajian, A., & Berglund, L. A. (2017). Nanostructured wood hybrids for fire-retardancy prepared by clay impregnation into the cell wall. ACS applied materials & interfaces, 9(41), 36154-36163.

[37] Fuentes-Sepúlveda, R., García-Herrera, C., Vasco, D. A., Salinas-Lira, C., & Ananías, R. A. (2020). Thermal characterization of Pinus radiata wood vacuum-impregnated with octadecane. Energies, 13(4), 942.

[38] Gao, X., Cai, J., Jin, J., & Zhuang, S. (2017). Bound water content and pore size diameter distribution in swollen cell walls determined by NMR cryoporometry. Journal of Nanjing Forestry University (Natural Sciences Edition), 41(2), 150-156.

[39] Giro-Paloma, J., Martínez, M., Cabeza, L. F., & Fernández, A. I. (2016). Types, methods, techniques, and applications for microencapsulated phase change materials (MPCM): A review. Renewable and Sustainable Energy Reviews, 53, 1059-1075.

[40] Grigsby, W. J., Kroese, H., & Dunningham, E. A. (2013). Characterisation of pore size distributions in variously dried Pinus radiata: analysis by thermoporosimetry. Wood Science and Technology, 47, 737–747.

[41] Guo, X., Cao, J., Peng, Y., & Liu, R. (2016). Incorporation of microencapsulated dodecanol into wood flour/high-density polyethylene composite as a phase change material for thermal energy storage. Materials & Design, 89, 1325-1334.

[42] Heng, Y., Feng, N., Liang, Y., & Hu, D. (2020). Lignin-retaining porous bamboo-based reversible thermochromic phase change energy storage composite material. International Journal of Energy Research, 44(7), 5441-5454.

[43] Hernandez-Charpak, Y. D., Trabold, T. A., Lewis, C. L., & Diaz, C. A. (2022). Biochar-filled plastics: Effect of feedstock on thermal and mechanical properties. Biomass Conversion and Biorefinery, 1-12.

[44] Jackson, C. L., & McKenna, G. B. (1990). The melting behavior of organic materials confined in porous solids, J. Chem. Phys., 93 (12), 9002–9011.

[45] Jamekhorshid, A., Sadrameli, S. M., Barzin, R., & Farid, M. M. (2017). Composite of wood-plastic and micro-encapsulated phase change material (MEPCM) used for thermal energy storage. Applied Thermal Engineering, 112, 82-88.

[46] Jebasingh, B. E., & Arasu, A. V. (2020). A detailed review on heat transfer rate, supercooling, thermal stability and reliability of nanoparticle dispersed organic phase change material for low-temperature applications. Materials Today Energy, 16, 100408.

[47] Jeon, J., Park, J. H., Wi, S., Yang, S., Ok, Y. S., & Kim, S. (2019). Latent heat storage biocomposites of phase change material-biochar as feasible eco-friendly building materials. Environmental research, 172, 637-648.

[48] Jeong, S. G., Jeon, J., Seo, J., Lee, J. H., & Kim, S. (2012). Performance evaluation of the microencapsulated PCM for wood-based flooring application. Energy conversion and management, 64, 516-521.

[49] Jiang, T., Zhang, Y., Olayiwola, S., Lau, C., Fan, M., Ng, K., & Tan, G. (2022). Biomass-derived porous carbons support in phase change materials for building energy efficiency: a review. Materials Today Energy, 23, 100905.

[50] Kane, S. D. (2022). Biochar as a renewable carbon additive for biodegradable plastics, Dissertation Doctorate of Philosophy, Montana State University, August 2022.

[51] Khadiran, T., Hussein, M. Z., Zainal, Z., & Rusli, R. (2015). Encapsulation techniques for organic phase change materials as thermal energy storage medium: A review. Solar Energy Materials and Solar Cells, 143, 78-98.

[52] Kojiro, K., Miki, T., Sugimoto, H., Nakajima, M., & Kanayama, K. (2010). Micropores and mesopores in the cell wall of dry wood. Journal of Wood Science, 56(2), 107-111.

[53] Kumar, A., Jyske, T., & Petrič, M. (2021). Delignified wood from understanding the hierarchically aligned cellulosic structures to creating novel functional materials: a review. Advanced Sustainable Systems, 5(5), 2000251.

[54] Landry, M. R. (2005). Thermoporometry by differential scanning calorimetry: experimental considerations and applications. Thermochimica acta, 433(1-2), 27-50.

[55] Lebo, S. E. Jr., Gargulak, J. D., McNally, Timothy J. (2001). "Lignin" in Kirk-Othmer Encyclopedia of Chemical Technology. John Wiley & Sons, Inc. doi:10.1002/0471238961

[56] Leng, L., Xiong, Q., Yang, L., Li, H., Zhou, Y., Zhang, W., Jiang, S., Li, H., & Huang, H. (2021). An overview on engineering the surface area and porosity of biochar. Science of the total Environment, 763, 144204.

[57] Lepak-Kuc, S., Kiciński, M., Michalski, P. P., Pavlov, K., Giorcelli, M., Bartoli, M., & Jakubowska, M. (2021). Innovative Biochar-Based Composite Fibres from Recycled Material. Materials, 14(18), 5304.

[58] Li, J., Xue, P., Ding, W., Han, J., & Sun, G. (2009). Micro-encapsulated paraffin/high-density polyethylene/wood flour composite as form-stable phase change material for thermal energy storage. Solar Energy Materials and Solar Cells, 93(10), 1761-1767.

[59] Li, Y., Fu, Q., Yu, S., Yan, M., & Berglund, L. (2016). Optically transparent wood from a nanoporous cellulosic template: combining functional and structural performance. Biomacromolecules, 17(4), 1358-1364.

[60] Li, Y., Fu, Q., Yang, X., & Berglund, L. (2018). Transparent wood for functional and structural applications. Philosophical Transactions of the Royal Society A: Mathematical, Physical and Engineering Sciences, 376(2112), 20170182.

[61] Li, Y., Vasileva, E., Sychugov, I., Popov, S., & Berglund, L. (2018). Optically transparent wood: Recent progress, opportunities, and challenges. Advanced Optical Materials, 6(14), 1800059.

[62] Liang, J., Zhimeng, L., Ye, Y., Yanjun, W., Jingxin, L., & Changlin, Z. (2018). Fabrication and characterization of fatty acid/wood-flour composites as novel form-stable phase change materials for thermal energy storage. Energy and Buildings, 171, 88-99.

[63] Liang, R., Zhu, Y. H., Wen, L., Zhao, W. W., Kuai, B. B., Zhang, Y. L., & Cai, L. P. (2020). Exploration of effect of delignification on the mesopore structure in poplar cell wall by nitrogen absorption method. Cellulose, 27(4), 1921-1932.

[64] Liu, S., Wu, H., Du, Y., Lu, X., & Qu, J. (2021). Shape-stable composite phase change materials encapsulated by bio-based balsa wood for thermal energy storage. Solar Energy Materials and Solar Cells, 230, 111187.

[65] Lyczakowski, J. J., Bourdon, M., Terrett, O. M., Helariutta, Y., Wightman, R., & Dupree, P. (2019). Structural imaging of native cryo-preserved secondary cell walls reveals the presence of macrofibrils

and their formation requires normal cellulose, lignin and xylan biosynthesis. Frontiers in plant science, 10, 1398.

[66] Ma, L., Guo, C., Ou, R., Sun, L., Wang, Q., & Li, L. (2018). Preparation and characterization of modified porous wood flour/lauric-myristic acid eutectic mixture as a form-stable phase change material. Energy & Fuels, 32(4), 5453-5461.

[67] Ma, L., Wang, Q., & Li, L. (2019). Delignified wood/capric acid-palmitic acid mixture stable-form phase change material for thermal storage. Solar Energy Materials and Solar Cells, 194, 215-221.

[68] Maljaee, H., Madadi, R., Paiva, H., Tarelho, L., & Ferreira, V. M. (2021). Incorporation of biochar in cementitious materials: A roadmap of biochar selection. Construction and Building Materials, 283, 122757.

[69] Meier, Eric (2022). Hardwood Anatomy, The Wood Database, www.wood-database.com/wood-articles/hardwood-anatomy/

[70] Meier, Eric (2022). Softwood Anatomy, The Wood Database, www.wood-database.com/wood-articles/softwood-anatomy/

[71] Meng, Y., Majoinen, J., Zhao, B., & Rojas, O. J. (2020). Form-stable phase change materials from mesoporous balsa after selective removal of lignin. Composites Part B: Engineering, 199, 108296.

[72] Minugu, O. P., Gujjala, R., Shakuntala, O., Manoj, P., & Chowdary, M. S. (2021). Effect of biomass derived biochar materials on mechanical properties of biochar epoxy composites. Proceedings of the Institution of Mechanical Engineers, Part C: Journal of Mechanical Engineering Science, 235(21), 5626-5638.

[73] Mitran, R. A., Berger, D., Munteanu, C., & Matei, C. (2015). Evaluation of different mesoporous silica supports for energy storage in shape-stabilized phase change materials with dual thermal responses. The Journal of Physical Chemistry C, 119(27), 15177-15184.

[74] Montanari, C., Li, Y., Chen, H., Yan, M., & Berglund, L. A. (2019). Transparent wood for thermal energy storage and reversible optical transmittance. ACS applied materials & interfaces, 11(22), 20465-20472.

[75] Montanari, C., Ogawa, Y., Olsén, P., & Berglund, L. A. (2021). High Performance, Fully Bio-Based, and Optically Transparent Wood Biocomposites. Advanced Science, 8(12), 2100559.

[76] Muthoka, R. M., Panicker, P. S., Agumba, D. O., Pham, H. D., & Kim, J. (2021). All-biobased transparent-wood: A new approach and its environmental-friendly packaging application. Carbohydrate Polymers, 264, 118012.

[77] Nakamura, K., Hatakeyama, T., & Hatakeyama, H. (1981). Studies on bound water of cellulose by differential scanning calorimetry. Textile Research Journal, 51, 607–613.

[78] Nam, J., Yun, B. Y., Choi, J. Y., & Kim, S. (2022). Potential of wood as thermal energy storage materials: Different characteristics depending on the hierarchical structure and components. International Journal of Energy Research, 46(11), 14926-14945.

[79] Nopens, M., Sazama, U., König, S., Kaschuro, S., Krause, A., & Fröba, M. (2020). Determination of mesopores in the wood cell wall at dry and wet state. Scientific Reports, 10(1), 1-11.

[80] Ok, Y. S., Uchimiya, S. M., Chang, S. X., & Bolan, N. (Eds.). (2015). Biochar: Production, characterization, and applications. CRC press.

[81] Ok, Y. S., Tsang, D. C., Bolan, N., & Novak, J. M. (Eds.). (2018). Biochar from biomass and waste: fundamentals and applications. Elsevier.

[82] Panahi, H. K. S., Dehhaghi, M., Ok, Y. S., Nizami, A. S., Khoshnevisan, B., Mussatto, S. I., Aghbashlo, M., Tabatabaei, M., & Lam, S. S. (2020). A comprehensive review of engineered biochar: production, characteristics, and environmental applications. Journal of cleaner production, 270, 122462.

[83] Papadopoulos, A. N., Bikiaris, D. N., Mitropoulos, A. C., & Kyzas, G. Z. (2019). Nanomaterials and chemical modifications for enhanced key wood properties: A review. Nanomaterials, 9(4), 607.

[84] Park, S., Venditti, R. A., Jameel, H., & Pawlak, J. J. (2006). Changes in pore size distribution during the drying of cellulose fibers as measured by differential scanning calorimetry. Carbohydrate polymers, 66(1), 97-103.

[85] Plötze, M., & Niemz, P. (2011). Porosity and pore size distribution of different wood types as determined by mercury intrusion porosimetry. European journal of wood and wood products, 69(4), 649-657.

[86] Rathod, M. K., & Banerjee, J. (2013). Thermal stability of phase change materials used in latent heat energy storage systems: A review. Renewable and sustainable energy reviews, 18, 246-258.

[87] Rathod, M. K. (2018). Thermal stability of phase change material. IntechOpen. DOI: 10.5772/intechopen.75923

[88] Rosenthal, M., & Bäucker, E. (2013). Zur Anatomie des Holzes der Weiß-Eichen: rasterelektronenmikroskopische Bildtafeln zu den drei holzanatomischen Schnittrichtungen. Technische Universität Dresden, Fakultät Umweltwissenschaften, Professur für Forstnutzung.

[89] Rosso, C., Das, O., & Bartoli, M. (2020). Insight into the mechanical performance of biochar containing reinforced plastics. In Biochar: Emerging applications. IOP Publishing.

[90] Saavedra, H., García-Herrera, C., Vasco, D. A., & Salinas-Lira, C. (2021). Characterization of mechanical performance of Pinus radiata wood impregnated with octadecane as phase change material. Journal of Building Engineering, 34, 101913.

[91] Salamon, D. (2014). Advanced ceramics. In Advanced ceramics for dentistry (pp. 103-122). Butterworth-Heinemann.

[92] Sawabe, O., Mori, K. & Takeuchi, T. (1973). Micro-pore structure in cell wall of wood. Mokuzai Gakkaishi, 2, 55–62.

[93] Sing, K. S. (1991). Characterization of porous solids: An introductory survey. In Studies in Surface Science and Catalysis (Vol. 62, pp. 1-9). Elsevier.

[94] Singh, B., Singh, B. P., & Cowie, A. L. (2010). Characterisation and evaluation of biochars for their application as a soil amendment. Soil Research, 48(7), 516-525.

[95] Singh, T., Arapanaei, A., Elustondo, D., Wang, Y., Stocchero, A., West, T., & Fu, Q. (2022). Emerging technologies for the development of wood products towards extended carbon storage and CO2 capture. Carbon Capture Science & Technology, 100057.

[96] Sirico, A., Bernardi, P., Sciancalepore, C., Vecchi, F., Malcevschi, A., Belletti, B., & Milanese, D. (2021). Biochar from wood waste as additive for structural concrete. Construction and Building Materials, 303, 124500.

[97] Sivanathan, A., Dou, Q., Wang, Y., Li, Y., Corker, J., Zhou, Y., & Fan, M. (2020). Phase change materials for building construction: An overview of nano-micro-encapsulation. Nanotechnology Reviews, 9(1), 896-921.

[98] Sparavigna, A. C., Giurdanella, S., & Patrucco, M. (2011). Behaviour of Thermodynamic Models with Phase Change Materials under Periodic Conditions. Energy and Power Engineering, 3(02), 150. DOI: 10.4236/epe.2011.32019

[99] Sparavigna, A. C. (2022). Biochar Shape-Stabilized Phase-Change Materials for Thermal Energy Storage. SSRN Electronic Journal. DOI: 10.2139/ssrn.4310141

[100] Spear, M. J., Curling, S. F., Dimitriou, A., & Ormondroyd, G. A. (2021). Review of functional treatments for modified wood. Coatings, 11(3), 327.

[101] Suarez-Riera, D., Lavagna, L., Bartoli, M., Giorcelli, M., Pavese, M., & Tagliaferro, A. (2022). The influence of biochar shape in cement-based materials. Magazine of Concrete Research, 1-13.

[102] Tan, K. H., Wang, T. Y., Zhou, Z. H., & Qin, Y. H. (2021). Biochar as a partial cement replacement material for developing sustainable concrete: An overview. Journal of Materials in Civil Engineering, 33(12), 03121001.

[103] Tian, S., Yang, R., Pan, Z., Su, X., Li, S., Wang, P., & Huang, X. (2022). Anisotropic reed-stem-derived hierarchical porous biochars supported paraffin wax for efficient solar-thermal energy conversion and storage. Journal of Energy Storage, 56, 106153.

[104] Toumpanaki, E., Shah, D. U., & Eichhorn, S. J. (2021). Beyond what meets the eye: Imaging and imagining wood mechanical–structural properties. Advanced Materials, 33(28), 2001613.

[105] Trisnadewi, T., & Putra, N. (2020, September). Phase change material (PCM) with shaped stabilized method for thermal energy storage: A review. In AIP Conference Proceedings (Vol. 2255, No. 1, p. 030065). AIP Publishing LLC.

[106] Tsoumis, G. (1991). Science and technology of wood: structure, properties, utilization (Vol. 115). New York: Van Nostrand Reinhold.

[107] Vitas, S., Segmehl, J. S., Burgert, I., & Cabane, E. (2019). Porosity and pore size distribution of native and delignified beech wood determined by mercury intrusion porosimetry. Materials, 12(3), 416.

[108] Wang, W., Cao, H., Liu, J., Jia, S., Ma, L., Guo, X., & Sun, W. (2020). A thermal energy storage composite by incorporating microencapsulated phase change material into wood. RSC advances, 10(14), 8097-8103.

[109] Wang, Q., Lai, Z., Luo, C., Zhang, J., Cao, X., Liu, J., & Mu, J. (2021). Honeycomb-like activated carbon with microporous nanosheets structure prepared from waste biomass cork for highly efficient dye wastewater treatment. Journal of Hazardous Materials, 416, 125896.

[110] Warnock, J., Awschalom, D. D., & Shafer, M. W. (1986). Geometrical supercooling of liquids in porous glass. Physical review letters, 57(14), 1753.

[111] Webber, J.B.W., Corbett, P., Semple, K.T., Ogbonnaya, U., Teel, W.S., Masiello, C.A., Fisher, Q.J., Valenza II, J.J., Song, Y.Q. & Hu, Q. (2013). An NMR study of porous rock and biochar containing organic material. Microporous and Mesoporous Materials, 178, pp.94-98.

[112] White, H. J., & Eyring, H. (1947). The Adsorption of Water by Swelling High Polyrneric Materials. Textile Research Journal, 17, 523–553.

[113] Willems, W. (2016). Equilibrium thermodynamics of wood moisture revisited: presentation of a simplified theory. Holzforschung, 70, 963–970.

[114] Wong, J. W. C., Webber, J. B. W., & Ogbonnaya, U. O. (2019). Characteristics of biochar porosity by NMR and study of ammonium ion adsorption. Journal of Analytical and Applied Pyrolysis, 143, 104687.

[115] Wool, R. P. (20011). Polymers and composite resins from plant oils. Bio-Based Polymers and Composites, Wool, R. P., & Susan Sun, X. S., Eds. Elsevier, 2011, ISBN 0080454348, 9780080454344

[116] Xu, L., Xiong, Y., Dang, B., Ye, Z., Jin, C., Sun, Q., & Yu, X. (2019). In-situ anchoring of Fe3O4/ZIF-67 dodecahedrons in highly compressible wood aerogel with excellent microwave absorption properties. Materials & Design, 182, 108006.

[117] Yang, H., Wang, Y., Yu, Q., Cao, G., Yang, R., Ke, J., Di, X., Liu, F., Zhang, W., & Wang, C. (2018). Composite phase change materials with good reversible thermochromic ability in delignified wood substrate for thermal energy storage. Applied energy, 212, 455-464.

[118] Yang, H., Chao, W., Di, X., Yang, Z., Yang, T., Yu, Q., Liu, F., Li, J., Li, G., & Wang, C. (2019). Multifunctional wood based composite phase change materials for magnetic-thermal and solar-thermal energy conversion and storage. Energy Conversion and Management, 200, 112029.

[119] Yin, S., Huang, Y., Deng, C., Jiao, Y., Wu, W., Seidi, F., & Xiao, H. (2022). Hierarchically porous biochar derived from orthometric integration of wooden and bacterial celluloses for high-performance electromagnetic wave absorption. Composites Science and Technology, 218, 109184.

[120] Zhang, Y. P., Lin, K. P., Yang, R., Di, H. F., & Jiang, Y. (2006). Preparation, thermal performance and application of shape-stabilized PCM in energy efficient buildings. Energy and buildings, 38(10), 1262-1269.

[121] Zhang, Y., He, M., Wang, L., Yan, J., Ma, B., Zhu, X., Ok, S. Y., Mechtcherine, V., & Tsang, D. C. (2022a). Biochar as construction materials for achieving carbon neutrality. Biochar, 4(1), 1-25.

[122] Zhang, Q., Liu, J., Zhang, J., Lin, L., & Shi, J. (2022b). A review of composite phase change materials based on biomass materials. Polymers, 14(19), 4089.

[123] Zhong, X., & Ma, E. (2022). A novel approach for characterizing pore size distribution of wood cell wall using differential scanning calorimetry thermoporosimetry. Thermochimica Acta, 718, 179380.

[124] Zhu, S., Biswas, S. K., Qiu, Z., Yue, Y., Fu, Q., Jiang, F., & Han, J. (2022). Transparent wood-based functional materials via a top-down approach. Progress in Materials Science, 101025.